Crystalline Polyphenylene Covalent Organic Frameworks

Xing Han [a,b], Zihui Zhou [a,b], Kaiyu Wang [a,b], Zhiling Zheng [a,b], S. Ephraim Neumann [a,b], Tianqiong Ma [a,b], and Omar M. Yaghi [a,b,c*]

[a] Department of Chemistry and Kavli Energy Nanoscience Institute, University of California, Berkeley, California 94720, United States.

[b] Bakar Institute of Digital Materials for the Planet, College of Computing, Data Science, and Society, University of California, Berkeley, California 94720, United States.

[c] KACST−UC Berkeley Center of Excellence for Nanomaterials for Clean Energy Applications, King Abdulaziz City for Science and Technology, Riyadh 11442, Saudi Arabia.

yaghi@berkeley.edu

ABSTRACT: The synthesis of crystalline polyphenylene covalent organic frameworks (COFs) was accomplished by linking fluorinated tris(4-acetylphenyl)benzene building units using aldol cyclotrimerization. The structures of two COFs, reported here, were confirmed by powder X-ray diffraction techniques, Fourier-transform infrared, and solid-state ^{13}C CP/MAS NMR spectroscopy. The results showed that the COFs were porous and chemically stable in corrosive, harsh environments for at least 1 week. Accordingly, post-synthetically modified derivatives of these COFs using primary amines showed CO_2 uptake from air and flue gas.

INTRODUCTION

The chemistry of covalent organic frameworks (COFs) has been largely dominated by structures made from highly reversible linkages such as imines,[1-4] boroxines,[5-6] and hydrazones,[7-8] Recently, COFs containing linkages considered irreversible have also been successfully crystallized, most notably, olefins,[9-11] sp^2-carbon,[12-15] truxenes,[16] triazines,[17-19] phenazines,[20-21] oxazoles,[22-23] and dioxins.[24-26] An important objective is to crystallize COFs based on C-C linkages, so that such structures could be deployed for many years in capturing carbon dioxide from air and flue gas, among many applications. We report the use of aldol cyclotrimerization (Figure 1a) to form polyphenylene COFs.

Specifically, the cyclotrimerization of 1,3,5-trifluoro-2,4,6-tris(4-acetylphenyl)benzene (TAB) or 1,3,5-trifluoro-2,4,6-tris(4-acetylphenylethynyl)benzene (TAEB) yields crystalline 2D frameworks with **hcb** topology, termed COF-284 and COF-285 (Figure 1b and 1c). The phenyl linkages of these COFs were unambiguously confirmed by Fourier transform infrared (FT-IR) spectroscopy and solid state ^{13}C cross-polarization magic angle spinning (CP-MAS) NMR spectroscopy. The irreversible phenyl linkage endows the COFs with exceptionally high stability under extreme chemical conditions. Following post-synthetic modification, alkyl amines can be anchored onto the COFs' backbone, resulting in a CO_2 uptake capacity at low pressure (0.4 mbar).

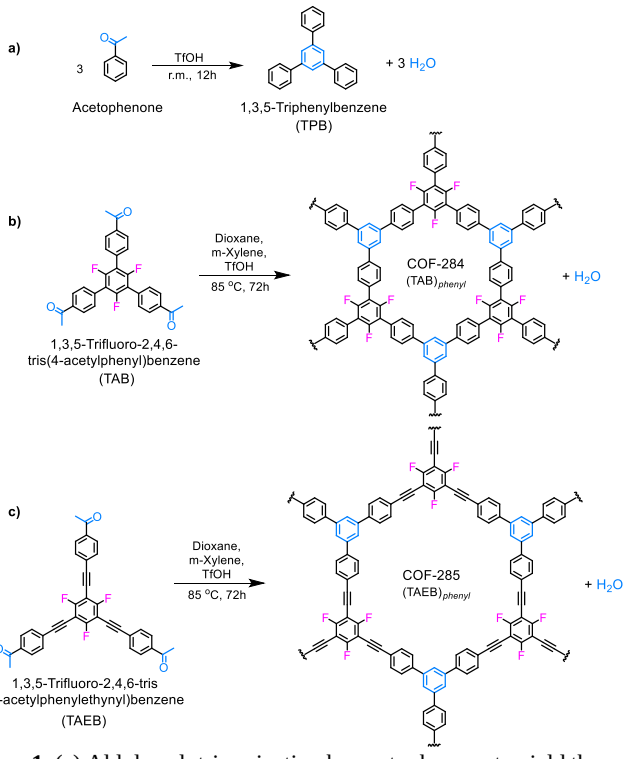

Figure 1. (a) Aldol cyclotrimerization by acetophenone to yield the model compound TPB. (b), (c) Synthesis of COF-284 and COF-285 by aldol cyclotrimerization with the fluorinated linkers TAB and TAEB.

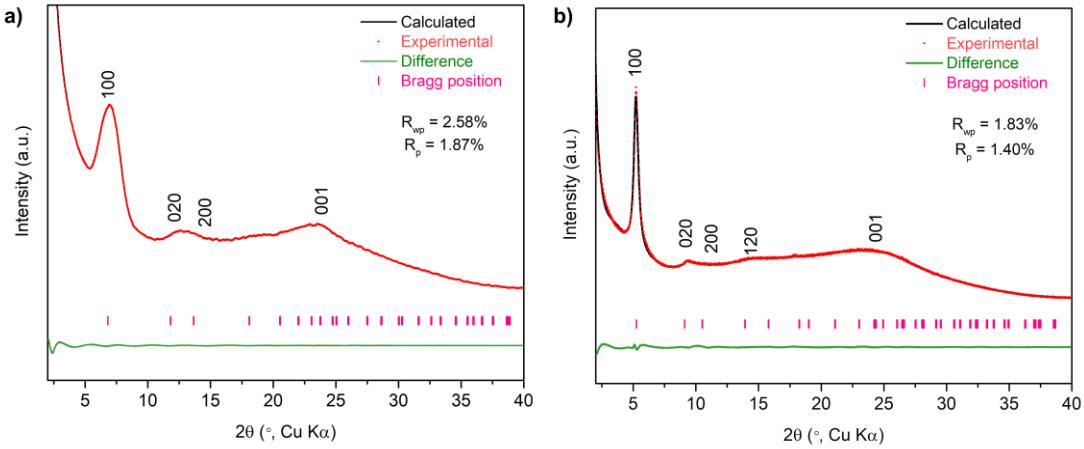

Figure 2. PXRD patterns and Pawley refinement of COF-284 (**a**) and COF-285 (**b**), respectively. The experimental pattern (red) is in good agreement with the eclipsed stacking model (black).

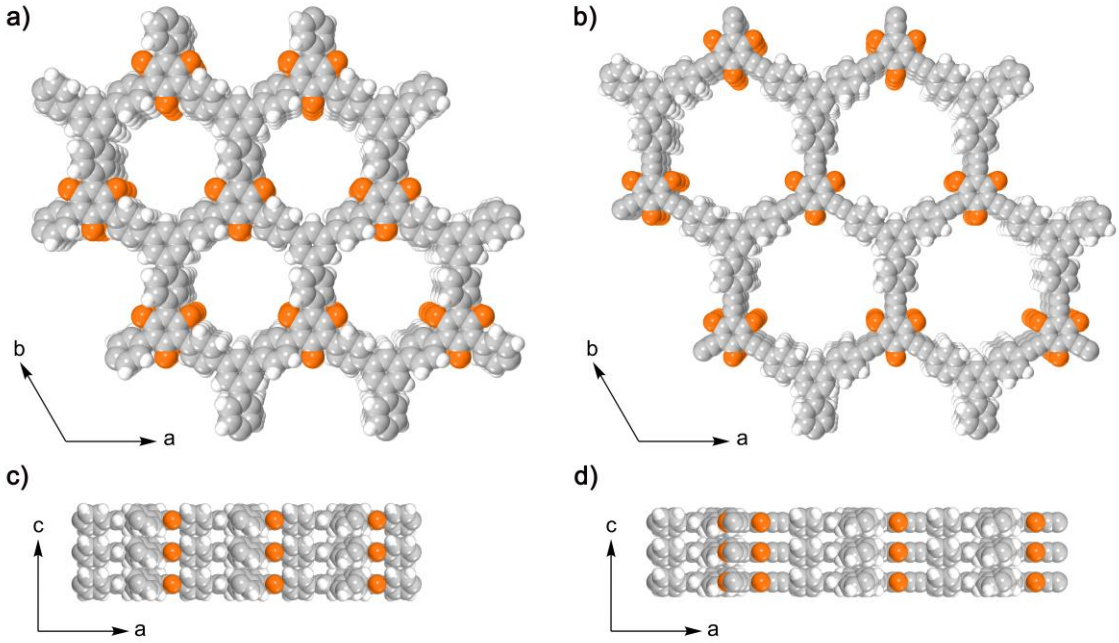

Figure 3. (a, b) Top views and (c, d) side views of the space-filling models of COF-284 and -285 in eclipsed stacking mode. Color code: H, white; C, gray; F, orange.

The molecular reaction of the aldol cyclotrimerization of acetophenone has been employed in the synthesis of a series of molecules and polymers (e.g., 1,3,5-Triphenylbenzene, TPB, Figure 1a). The reaction is typically performed in the presence of a strong Brønsted acid.[27-28] However, direct application of these reaction conditions to the synthesis of COFs results, as expected, in the formation of amorphous materials, indicating insufficient reversibility for defect correction.[29-30] Extensive efforts were applied to screen various synthetic conditions including linkers, solvent mixtures, temperature, and reaction time. For reactions that exhibit irreversible characteristics and, therefore, lack the ability to self-correct defects, careful modulation of the reaction conditions is crucial to reduce the reaction rate. This ensures that linkers connect slowly enough to assemble and stack in an orderly fashion, thus yielding a crystalline structure. However, a common trade-off with this approach is a potential reduction in reaction yield. A crystalline framework, termed COF-284, was successfully synthesized under solvothermal conditions in a mixture of 1,4-dioxane, and *m*-xylene, with aqueous trifluoromethanesulfonic acid (TfOH) as a catalyst at 85 °C for 72 hours in moderate yield (32%) (Section S2.6).

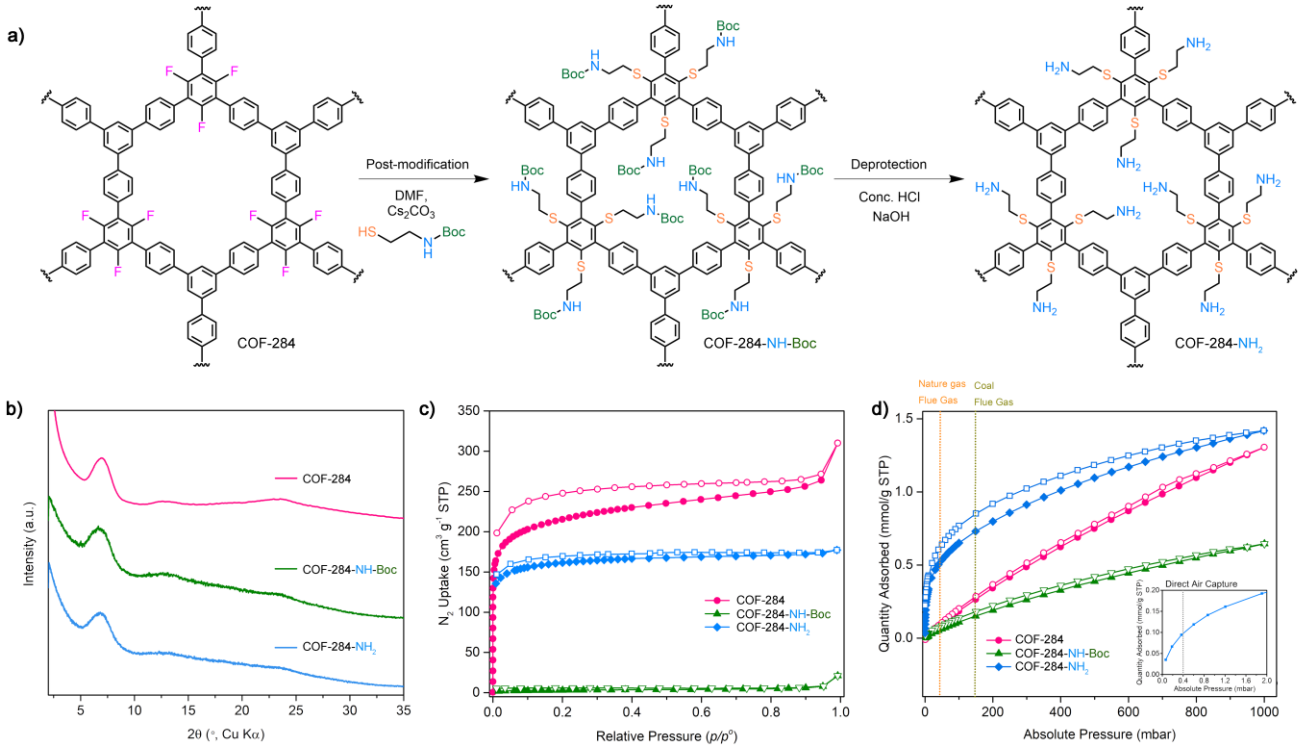

Figure 4. (a) Schematics of the synthesis of COF-284-NH_2, (b) PXRD patterns, (c) N_2 sorption isotherms (77 K), and (d) single component CO_2 isotherms (25 °C) of COFs. The inset in panel (d) displays a zoomed-in view of the adsorption branch of COF-284-NH_2 at 0-2 mbar to highlight the uptake at the DAC-relevant pressure.

In this process, we applied a strategy that combined an initial human-centric screening with subsequent machine learning-guided synthesis condition optimization (Section S2.10),[31-36] efficiently pinpointing optimal conditions from a vast potential space of combinations.[37] These combinations stemmed from seven key synthesis parameters associated with the crystallization of COF-284 (Table S1 and S2).[38] This balanced methodology enhances efficiency, diminishes human bias, and adeptly navigates between exploration and exploitation of optimal conditions. We further extended the reaction scope by crystallizing COF-285 through cyclotrimerization of TAEB using similar conditions. COF-284 and -285 were obtained as pale yellow or red microcrystalline powders, insoluble in common organic solvents such as dichloromethane, acetone, alcohols, tetrahydrofuran, and *N*,*N*-dimethylformamide. It should be noted that incorporating fluorine substituents onto the periphery of the COFs' building units plays an important role in the ability to crystallize these structures. We hypothesized that fluorine being an electron-withdrawing group enhances aromatic stacking interactions without introducing significant steric effects.[39] The non-fluorinated analogous building blocks only form amorphous solids under similar synthetic conditions (Figure S15).

In the Fourier-transform infrared (FT-IR) spectra of COF-284 and COF-285, the peaks attributed to the C=O and C-H stretching of the acetyl linkers, found at approximately 1680 cm^{-1} and 3040 cm^{-1}, respectively, are markedly reduced compared to the spectra of TAB and TAEB (Figures S3 and S4). Concurrently, there is an increased intensity at approximately 1600 cm^{-1}, corresponding to the aromatic C=C stretch in the phenyl ring formed during the COF synthesis. The residual C=O stretch at 1686 to 1688 cm^{-1} can be assigned to the defects and intermediates formed during the COF's synthesis. Further support for the presence of the phenyl linkages was obtained by solid-state ^{13}C cross-polarization magic angle spinning (CP-MAS) NMR analysis. The ^{13}C CP-MAS NMR spectra of COF-284 and COF-285 revealed the almost complete disappearance of signals at chemical shifts of 195 ppm and 25 ppm, which correspond to the carbonyl and alkyl carbons of the acetyl group, respectively (Figures S6 and S7). Although there is an overlap of aromatic carbon signals between the linkage and the backbone, an increased peak intensity at 126 ppm was observed, which is attributed to the newly formed phenyl rings.

The crystallinity of COF-284 and COF-285 was confirmed by Powder X-ray diffraction (PXRD) (Figure 2). Based on the planar geometry of the model compound TPB and its analogs in single-crystal structures, structural models of COF-284 and COF-285 were constructed based on an **hcb** topology. Several interlayer stacking modes were modeled and compared to the experimental PXRD pattern, among which the model with an eclipsed (AA) stacking mode in space group *P*3 provided the best fit (Figures S13 and S14). Full profile Pawley refinement of the model against the experimental pattern yielded a unit cell parameters of $a = b$ =14.98Å and c = 4.01 Å, $\alpha = \beta = 90°$, $\gamma = 120°$ with good agreement factors (R_{wp} = 2.58%, R_p = 1.87%) for COF-284 and $a = b$ = 19.44 Å and c = 3.65 Å, $\alpha = \beta = 90°$, $\gamma = 120°$ with agreement factors (R_{wp} = 1.83%, R_p = 1.40%) for COF-285, respectively.

The porosity and surface areas of COF-284 and COF-285 were evaluated after removal of solvent molecules from the pores by activation in *vacuo*. The N_2 sorption isotherm measurements performed on COF-284 and COF-285 at 77 K revealed that the pores of the two COFs were accessible to N_2, with a Brunauer-Emmett-Teller (BET) surface area of 812 $m^2 g^{-1}$ and 395 $m^2 g^{-1}$, respectively (Figures 4c, S16 and S17). Fitting of the isotherm based on non-local density functional theory indicated a uniform pore size distribution featuring a narrow peak at 9.2 Å and 12.6 Å diameter, respectively, which is close to the expected 9.3 Å and 13.0 Å based on the calculated van der Waals surface of the structural model (Figure S18).

The thermal stability of COF-284 and COF-285 was evaluated using thermogravimetric analysis. Both COFs exhibited high thermal stability, showing no significant weight loss up to 400 °C under an N_2 atmosphere (Figure S11). To evaluate the chemical stability of the polyphenylene COFs, the materials were exposed to a series of organic and inorganic Brønsted acids and bases. Specifically, the activated COFs were suspended in 12.1 mol L^{-1} aqueous HCl (35 wt%), trifluoromethanesulfonic acid (≥99%), H_2SO_4 (98 wt%), saturated aqueous KOH (55 wt%), and saturated methanolic KOH (35 wt%) at room temperature for 1 week. The structural integrity of the treated COF powders was examined by PXRD (Figure 5). The framework structures were found to maintain their crystallinity under all conditions. This is evidenced by the fact that the PXRD patterns of all treated samples remained largely unchanged in shape and intensity. Notably, the stability of the COFs to aqueous acid or base solutions can also be attributed to the hydrophobic nature of the materials. As such, COF-284 and COF-285 were suspended in pure TfOH, H_2SO_4, and saturated solutions of KOH in methanol, in which the materials still retained their crystallinity. The fact that the two COFs remain intact even under such harsh conditions for this length of time suggests significant chemical stability.

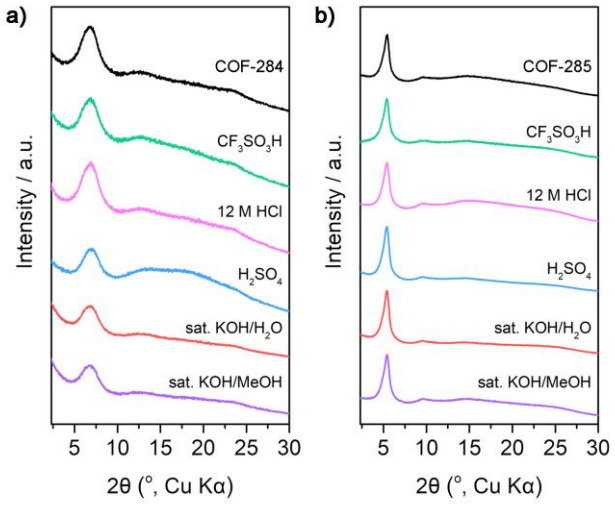

Figure 5. Chemical stability test of (a) COF-284 and (b) COF-285 with Brønsted acid and base. PXRD patterns of treated materials illustrate the retention of crystallinity of COFs under these very harsh conditions.

To utilize the exceptional stability and accessible fluorine functionalities, we developed a post-synthetic modification process to generate open amine groups within the pores of COF-284. The fluoride groups undergo a substitution reaction with 2-(Boc-amino) ethanthiol that decorates the channel walls with Boc-protected alkyl amines (Figures S5 and S8). The COF-284-NH-Boc can be readily deprotected using HCl, which results in the exposure of the corresponding amines, producing COF-284-NH_2. The PXRD patterns of the post-modification product showed only a slight decrease in crystallinity (Figures 4a, b), which can be attributed to the rigid backbone of the framework. The apparent decrease in the N_2 isotherm of COF-284-NH-Boc can be attributed to the introduced functional groups that block the pores of the framework (Figure 4c). After the Boc group was deprotected during the amination step, the porosity of material was partially restored, resulting in a BET surface area of 625 $m^2 g^{-1}$ for COF-284-NH_2.

Single-component CO_2 sorption isotherms of COF-284 before and after post-modification were measured at 25 °C and compared as shown in Figure 4d. For COF-284, the lack of a sharp uptake in the low-pressure region and a minimal hysteresis indicated that the framework has physisorption-dominant characteristics. COF-284-NH-Boc exhibited lower CO_2 uptake in the entire range of experiment (0-1000 mbar), which was attributed to the blocked pores after post-modification. In contrast, the CO_2 sorption isotherm of COF-284-NH_2 displayed a steep rise in the adsorption branch at very low CO_2 pressures, turning into a moderate slope between 50 and 1000 mbar, and a hysteresis between the adsorption and desorption branches. Specifically, COF-284-NH_2 adsorbs 2.2 $cm^3 g^{-1}$ STP (0.10 mmol g^{-1}) at 0.4 mbar CO_2 (conditions relevant to DAC) (Figure 4d, the inset), whereas COF-284, and COF-284-NH-Boc isotherms, as expected, did not take up any CO_2 at such a low concentration. At 40 mbar (relevant to post-combustion capture from natural gas flue), COF-284-NH_2 adsorbs 11.2 $cm^3 g^{-1}$ STP (0.5 mmol g^{-1}) CO_2, a 6-fold increase from COF-284 (1.79 $cm^3 g^{-1}$ STP, 0.08 mmol g^{-1}). At 150 mbar (relevant to post-combustion capture from coal flue gas), the CO_2 uptake of COF-284-NH_2 (16.6 $cm^3 g^{-1}$ STP, 0.74 mmol g^{-1}) is 3-fold higher than that of COF-284 (5.6 $cm^3 g^{-1}$ STP, 0.25 mmol g^{-1}). The significant increase of CO_2 uptake provided strong evidence that the introduction of chemisorption through incorporating aliphatic amines into COFs points to their potential as sorbents for efficient DAC and post-combustion capture (Figures S9 and S10).

ASSOCIATED CONTENT

Supporting Information

The Supporting Information is available free of charge at https://pubs.acs.org/doi/.

Detailed experimental section, Characterization including X-ray diffraction, Fourier-transform infrared spectroscopy, solid-state nuclear magnetic resonance spectroscopy, and thermogravimetric analysis (PDF).

Accession Codes

Crystallographic data for the two crystals reported in this communication have been deposited at the Cambridge Crystallographic Data Centre, under deposition numbers CCDC 2301434 (COF-

284), 2301435 (COF-285). These data can be obtained free of charge via www.ccdc.cam.ac.uk/data_request/cif, or by emailing data_request@ccdc.cam.ac.uk, or by contacting The Cambridge Crystallographic Data Centre, 12 Union Road, Cambridge CB2 1EZ, UK; fax: +44 1223 336033.

Notes

The authors declare no competing financial interest.

ACKNOWLEDGMENT

This research was supported by King Abdulaziz City for Science and Technology (KACST) as part of a joint KACST-UC Berkeley Center of Excellence for Nanomaterials for Clean Energy Applications. The authors thank the University of California Berkeley Electron Microscope Laboratory for access and assistance in electron microscopy data collection. We thank Drs. Hasan Celik, Raynald Giovine, and UC Berkeley's NMR facility in the College of Chemistry (CoC-NMR) for spectroscopic assistance. The instrument used in this work is supported by the National Science Foundation under Grant No. 2018784 and NIH S10OD024998.

REFERENCES

1. Ding, S.-Y.; Gao, J.; Wang, Q.; Zhang, Y.; Song, W.-G.; Su, C.-Y.; Wang, W., Construction of Covalent Organic Framework for Catalysis: Pd/COF-LZU1 in Suzuki–Miyaura Coupling Reaction. *J. Am. Chem. Soc.* **2011,** *133* (49), 19816-19822.
2. Natraj, A.; Ji, W.; Xin, J.; Castano, I.; Burke, D. W.; Evans, A. M.; Strauss, M. J.; Ateia, M.; Hamachi, L. S.; Gianneschi, N. C.; Alothman, Z. A.; Sun, J.; Yusuf, K.; Dichtel, W. R., Single-Crystalline Imine-Linked Two-Dimensional Covalent Organic Frameworks Separate Benzene and Cyclohexane Efficiently. *J. Am. Chem. Soc.* **2022,** *144* (43), 19813-19824.
3. Ma, T.; Kapustin, E. A.; Yin, S. X.; Liang, L.; Zhou, Z.; Niu, J.; Li, L.-H.; Wang, Y.; Su, J.; Li, J.; Wang, X.; Wang, W. D.; Wang, W.; Sun, J.; Yaghi, O. M., Single-crystal x-ray diffraction structures of covalent organic frameworks. *Science* **2018,** *361* (6397), 48-52.
4. Sun, T.; Wei, L.; Chen, Y.; Ma, Y.; Zhang, Y.-B., Atomic-Level Characterization of Dynamics of a 3D Covalent Organic Framework by Cryo-Electron Diffraction Tomography. *J. Am. Chem. Soc.* **2019,** *141* (28), 10962-10966.
5. Côté, A. P.; Benin, A. I.; Ockwig, N. W.; O'Keeffe, M.; Matzger, A. J.; Yaghi, O. M., Porous, Crystalline, Covalent Organic Frameworks. *Science* **2005,** *310* (5751), 1166-1170.
6. El-Kaderi, H. M.; Hunt, J. R.; Mendoza-Cortés, J. L.; Côté, A. P.; Taylor, R. E.; O'Keeffe, M.; Yaghi, O. M., Designed Synthesis of 3D Covalent Organic Frameworks. *Science* **2007,** *316* (5822), 268-272.
7. Uribe-Romo, F. J.; Doonan, C. J.; Furukawa, H.; Oisaki, K.; Yaghi, O. M., Crystalline Covalent Organic Frameworks with Hydrazone Linkages. *J. Am. Chem. Soc.* **2011,** *133* (30), 11478-11481.
8. Stegbauer, L.; Schwinghammer, K.; Lotsch, B. V., A hydrazone-based covalent organic framework for photocatalytic hydrogen production. *Chemical Science* **2014,** *5* (7), 2789-2793.
9. Xu, J.; He, Y.; Bi, S.; Wang, M.; Yang, P.; Wu, D.; Wang, J.; Zhang, F., An Olefin-Linked Covalent Organic Framework as a Flexible Thin-Film Electrode for a High-Performance Micro-Supercapacitor. *Angew. Chem. Int. Ed.* **2019,** *58* (35), 12065-12069.
10. Lyu, H.; Diercks, C. S.; Zhu, C.; Yaghi, O. M., Porous Crystalline Olefin-Linked Covalent Organic Frameworks. *J. Am. Chem. Soc.* **2019,** *141* (17), 6848-6852.
11. Wei, S.; Zhang, F.; Zhang, W.; Qiang, P.; Yu, K.; Fu, X.; Wu, D.; Bi, S.; Zhang, F., Semiconducting 2D Triazine-Cored Covalent Organic Frameworks with Unsubstituted Olefin Linkages. *J. Am. Chem. Soc.* **2019,** *141* (36), 14272-14279.
12. Chen, R.; Shi, J.-L.; Ma, Y.; Lin, G.; Lang, X.; Wang, C., Designed Synthesis of a 2D Porphyrin-Based sp2 Carbon-Conjugated Covalent Organic Framework for Heterogeneous Photocatalysis. *Angew. Chem. Int. Ed.* **2019,** *58* (19), 6430-6434.
13. Yuan, C.; Jia, W.; Yu, Z.; Li, Y.; Zi, M.; Yuan, L.-M.; Cui, Y., Are Highly Stable Covalent Organic Frameworks the Key to Universal Chiral Stationary Phases for Liquid and Gas Chromatographic Separations? *J. Am. Chem. Soc.* **2022,** *144* (2), 891-900.
14. Wang, S.; Li, X.-X.; Da, L.; Wang, Y.; Xiang, Z.; Wang, W.; Zhang, Y.-B.; Cao, D., A Three-Dimensional sp2 Carbon-Conjugated Covalent Organic Framework. *J. Am. Chem. Soc.* **2021,** *143* (38), 15562-15566.
15. Jin, E.; Asada, M.; Xu, Q.; Dalapati, S.; Addicoat, M. A.; Brady, M. A.; Xu, H.; Nakamura, T.; Heine, T.; Chen, Q., Two-dimensional sp2 carbon–conjugated covalent organic frameworks. *Science* **2017,** *357* (6352), 673-676.
16. Zhang, Q.; Sun, Y.; Li, H.; Tang, K.; Zhong, Y.-W.; Wang, D.; Guo, Y.; Liu, Y., Synthesis of Two-Dimensional C–C Bonded Truxene-Based Covalent Organic Frameworks by Irreversible Brønsted Acid-Catalyzed Aldol Cyclotrimerization. *Research* **2021,** *2021*.
17. Kuhn, P.; Antonietti, M.; Thomas, A., Porous, Covalent Triazine-Based Frameworks Prepared by Ionothermal Synthesis. *Angew. Chem. Int. Ed.* **2008,** *47* (18), 3450-3453.
18. Wang, K.; Yang, L.-M.; Wang, X.; Guo, L.; Cheng, G.; Zhang, C.; Jin, S.; Tan, B.; Cooper, A., Covalent Triazine Frameworks via a Low-Temperature Polycondensation Approach. *Angew. Chem. Int. Ed.* **2017,** *56* (45), 14149-14153.
19. Sun, T.; Liang, Y.; Xu, Y., Rapid, Ordered Polymerization of Crystalline Semiconducting Covalent Triazine Frameworks. *Angew. Chem. Int. Ed.* **2022,** *61* (4), e202113926.
20. Vitaku, E.; Gannett, C. N.; Carpenter, K. L.; Shen, L.; Abruña, H. D.; Dichtel, W. R., Phenazine-Based Covalent Organic Framework Cathode Materials with High Energy and Power Densities. *J. Am. Chem. Soc.* **2020,** *142* (1), 16-20.
21. Huang, N.; Lee, K. H.; Yue, Y.; Xu, X.; Irle, S.; Jiang, Q.; Jiang, D., A Stable and Conductive Metallophthalocyanine Framework for Electrocatalytic Carbon Dioxide Reduction in Water. *Angew. Chem. Int. Ed.* **2020,** *59* (38), 16587-16593.
22. Waller, P. J.; AlFaraj, Y. S.; Diercks, C. S.; Jarenwattananon, N. N.; Yaghi, O. M., Conversion of Imine to Oxazole and Thiazole Linkages in Covalent Organic Frameworks. *J. Am. Chem. Soc.* **2018,** *140* (29), 9099-9103.
23. Seo, J.-M.; Noh, H.-J.; Jeong, H. Y.; Baek, J.-B., Converting Unstable Imine-Linked Network into Stable Aromatic Benzoxazole-Linked One via Post-oxidative Cyclization. *J. Am. Chem. Soc.* **2019,** *141* (30), 11786-11790.
24. Zhang, B.; Wei, M.; Mao, H.; Pei, X.; Alshmimri, S. A.; Reimer, J. A.; Yaghi, O. M., Crystalline Dioxin-Linked Covalent Organic Frameworks from Irreversible Reactions. *J. Am. Chem. Soc.* **2018,** *140* (40), 12715-12719.

25. Lu, M.; Zhang, M.; Liu, C.-G.; Liu, J.; Shang, L.-J.; Wang, M.; Chang, J.-N.; Li, S.-L.; Lan, Y.-Q., Stable Dioxin-Linked Metallophthalocyanine Covalent Organic Frameworks (COFs) as Photo-Coupled Electrocatalysts for CO2 Reduction. *Angew. Chem. Int. Ed.* **2021,** *60* (9), 4864-4871.
26. Guan, X.; Li, H.; Ma, Y.; Xue, M.; Fang, Q.; Yan, Y.; Valtchev, V.; Qiu, S., Chemically stable polyarylether-based covalent organic frameworks. *Nat. Chem.* **2019,** *11* (6), 587-594.
27. Rose, M.; Klein, N.; Senkovska, I.; Schrage, C.; Wollmann, P.; Böhlmann, W.; Böhringer, B.; Fichtner, S.; Kaskel, S., A new route to porous monolithic organic frameworks via cyclotrimerization. *J. Mater. Chem.* **2011,** *21* (3), 711-716.
28. Lopez-Iglesias, B.; Suárez-García, F.; Aguilar-Lugo, C.; González Ortega, A.; Bartolomé, C.; Martínez-Ilarduya, J. M.; de la Campa, J. G.; Lozano, Á. E.; Álvarez, C., Microporous Polymer Networks for Carbon Capture Applications. *ACS Appl. Mater. Interfaces* **2018,** *10* (31), 26195-26205.
29. Zhu, X.; Tian, C.; Chai, S.; Nelson, K.; Han, K. S.; Hagaman, E. W.; Veith, G. M.; Mahurin, S. M.; Liu, H.; Dai, S., New Tricks for Old Molecules: Development and Application of Porous N-doped, Carbonaceous Membranes for CO2 Separation. *Adv. Mater.* **2013,** *25* (30), 4152-4158.
30. Zhao, Y.-C.; Zhou, D.; Chen, Q.; Zhang, X.-J.; Bian, N.; Qi, A.-D.; Han, B.-H., Thionyl Chloride-Catalyzed Preparation of Microporous Organic Polymers through Aldol Condensation. *Macromolecules* **2011,** *44* (16), 6382-6388.
31. Gongora, A. E.; Xu, B.; Perry, W.; Okoye, C.; Riley, P.; Reyes, K. G.; Morgan, E. F.; Brown, K. A., A Bayesian experimental autonomous researcher for mechanical design. *Sci. Adv.* **2020,** *6* (15), eaaz1708.
32. Langner, S.; Häse, F.; Perea, J. D.; Stubhan, T.; Hauch, J.; Roch, L. M.; Heumueller, T.; Aspuru-Guzik, A.; Brabec, C. J., Beyond Ternary OPV: High-Throughput Experimentation and Self-Driving Laboratories Optimize Multicomponent Systems. *Adv. Mater.* **2020,** *32* (14), 1907801.
33. Wahab, H.; Jain, V.; Tyrrell, A. S.; Seas, M. A.; Kotthoff, L.; Johnson, P. A., Machine-learning-assisted fabrication: Bayesian optimization of laser-induced graphene patterning using in-situ Raman analysis. *Carbon* **2020,** *167*, 609-619.
34. Xie, Y.; Zhang, C.; Deng, H.; Zheng, B.; Su, J.-W.; Shutt, K.; Lin, J., Accelerate Synthesis of Metal–Organic Frameworks by a Robotic Platform and Bayesian Optimization. *ACS Appl. Mater. Interfaces* **2021,** *13* (45), 53485-53491.
35. Burger, B.; Maffettone, P. M.; Gusev, V. V.; Aitchison, C. M.; Bai, Y.; Wang, X.; Li, X.; Alston, B. M.; Li, B.; Clowes, R.; Rankin, N.; Harris, B.; Sprick, R. S.; Cooper, A. I., A mobile robotic chemist. *Nature* **2020,** *583* (7815), 237-241.
36. Häse, F.; Roch, L. M.; Kreisbeck, C.; Aspuru-Guzik, A., Phoenics: A Bayesian Optimizer for Chemistry. *ACS Cent. Sci.* **2018,** *4* (9), 1134-1145.
37. Jones, D. R.; Schonlau, M.; Welch, W. J., Efficient Global Optimization of Expensive Black-Box Functions. *J. Glob. Optim.* **1998,** *13* (4), 455-492.
38. Haase, F.; Lotsch, B. V., Solving the COF trilemma: towards crystalline, stable and functional covalent organic frameworks. *Chem. Soc. Rev.* **2020,** *49* (23), 8469-8500.
39. Alahakoon, S. B.; McCandless, G. T.; Karunathilake, A. A. K.; Thompson, C. M.; Smaldone, R. A., Enhanced Structural Organization in Covalent Organic Frameworks Through Fluorination. *Chem. Eur. J.* **2017,** *23* (18), 4255-4259.

Table of Contents